

The mitochondrial genome of the red icefish  
(*Channichthys rugosus*) casts doubt on its  
species status

Moritz Muschick<sup>1,2\*</sup>, Ekaterina Nikolaeva<sup>3</sup>, Lukas Rüber<sup>1,4</sup>  
and Michael Matschiner<sup>5\*</sup>

<sup>1\*</sup>Aquatic Ecology & Evolution, Institute of Ecology and  
Evolution, University of Bern, Bern, 3012, Switzerland.

<sup>2</sup>Department of Fish Ecology & Evolution, EAWAG, Swiss  
Federal Institute for Aquatic Science and Technology,  
Kastanienbaum, 6047, Switzerland.

<sup>3</sup>Ichthyology Laboratory, Zoological Institute of the Russian  
Academy of Sciences, St. Petersburg, 199034, Russia.

<sup>4</sup>Naturhistorisches Museum Bern, Bern, 3005, Switzerland.

<sup>5</sup>Natural History Museum, University of Oslo, Oslo, 0562, Norway.

\*Corresponding author(s). E-mail(s): [Moritz.Muschick@eawag.ch](mailto:Moritz.Muschick@eawag.ch);  
[michael.matschiner@nhm.uio.no](mailto:michael.matschiner@nhm.uio.no);

Contributing authors: [ekaterina.nikolaeva@zin.ru](mailto:ekaterina.nikolaeva@zin.ru);  
[lukas.ruber@nmbe.ch](mailto:lukas.ruber@nmbe.ch);

### Abstract

Antarctic notothenioid fishes are recognized as one of the rare examples of adaptive radiation in the marine system. Withstanding the freezing temperatures of Antarctic waters, these fishes have diversified into over 100 species within no more than 10-20 million years. However, the exact species richness of the radiation remains contested. In the genus *Channichthys*, between one and nine species are recognized by different authors. To resolve the number of *Channichthys* species, genetic information would be highly valuable; however, so far, only sequences of a single species, *C. rhinoceratus*, are available. Here, we present the nearly complete sequence of the mitochondrial genome of *C. rugosus*, obtained from a formalin-fixed museum specimen sampled in 1974. This sequence

2 *Mitochondrial genome of the red icefish*

047 differs from the mitochondrial genome of *C. rhinoceratus* in no more  
 048 than 27 positions, suggesting that the two species may be synonymous.

049 **Keywords:** icefish, Antarctica, species richness, taxonomy, museomics,  
 050 mitochondrial genome

051  
 052  
 053  
 054

## 1 Introduction

056 The diversification of fishes of the perciform suborder Notothenioidei in  
 057 Antarctic waters is a rare example of adaptive radiation in the marine envi-  
 058 ronment (Clarke & Johnston, 1996; Eastman, 2005; Matschiner et al., 2015;  
 059 Near et al., 2012; Rüber & Zardoya, 2005). The radiating group of noto-  
 060 thenioid fishes is composed of five families (Nototheniidae, Harpagiferidae,  
 061 Artedidraconidae, Bathydraconidae, and Channichthyidae; jointly called "Cry-  
 062 onotothenioidea" (Near et al., 2015)) that together include over 100 species,  
 063 distributed primarily on the shelf areas surrounding Antarctica and sub-  
 064 Antarctic islands (Eastman & Eakin, 2021; Gon & Heemstra, 1990). The  
 065 validity of most species within this radiation is well established and in many  
 066 cases corroborated by genetic data. However, in other cases, species are known  
 067 only from few specimens and distinguished from congeners based on minute  
 068 morphological differences alone. One such example is the genus *Pogonophryne*  
 069 (Artedidraconidae), for which close to twenty species have been described  
 070 within the last four decades (Eastman & Eakin, 2021), primarily on the basis of  
 071 variation in the morphology of the mental barbel (*e.g.* Spodareva & Balushkin,  
 072 2014). This species richness within *Pogonophryne* could not be confirmed in a  
 073 recent genetic analysis, which instead led to the synonymization of 24 out of  
 074 29 valid species (Parker, Dornburg, Struthers, Jones, & Near, 2022).

075 Outside *Pogonophryne*, the validity of species described in the genus *Chan-*  
 076 *nichthys* (Channichthyidae) remains particularly questionable. As many as  
 077 nine species have been recognized, including the unicorn icefish (*C. rhinocera-*  
 078 *tus* Richardson, 1844), the red icefish (*C. rugosus* Regan, 1913), the sailfin pike  
 079 (*C. velifer* Meisner, 1974), and six species described by Shandikov between  
 080 1995 and 2011 (Aelita icefish, *C. aelitae*; big-eyed icefish, *C. bospori*; pygmy  
 081 icefish, *C. irinae*; charcoal icefish, *C. panticapaei*; green icefish, *C. mithridatis*;  
 082 and robust icefish, *C. richardsoni*) (Shandikov, 1995a, 1995b, 2008, 2011)  
 083 (Table 1). All species of the genus are endemic to the Kerguelen-Heard plateau  
 084 and appear to share largely overlapping distributions (Shandikov, 2011), im-  
 085 plying that they either represent a small radiation on their own, or that at  
 086 least some of the described taxa are *de facto* morphs of one and the same  
 087 species. The members of the genus are morphologically similar, with total  
 088 lengths around 30–50 cm, a wide and spatulated snout, a tall first dorsal fin,  
 089 and the rostral spine that gave its name to the the first described species, *C.*  
 090 *rhinoceratus* (Richardson, 1844).

091  
 092

The second-oldest species, *C. rugosus*, was described on the basis of two specimens that were found to differ from the known *C. rhinocerus* specimens in eye diameter, roughness of the head, the position of supraorbital edges, and the length of the maxillary (Regan, 1913). As additional specimens became available, the diagnosis of the two species became refined (Norman, 1937), but the lack of clearly species-defining traits led some authors to question their separation even before further members of the genus were described (Hureau, 1964). The third species to be described was *C. velifer* (Meisner, 1974), which was claimed to differ from *C. rhinocerus* in the number of spines of the first dorsal fin and the presence of a single median series of bony plates on the posterior part of the body (Meisner, 1974). However, most of the specimens assigned to this new taxon were females, suggesting that sexual dimorphism could have explained the observed differences (Gon & Heemstra, 1990). The six remaining described species were added to the list to accommodate previously unseen combinations of ray numbers, interorbital width, fin membrane height, and a duplicated row of gill rakers, among others (Shandikov, 1995a, 1995b, 2008, 2011). In most cases, these species were described on the basis of few specimens only.

**Table 1** Species described in genus *Channichthys*

Name	Authority	Year	# specimens
<i>C. rhinocerus</i>	Richardson	1844	1,093
<i>C. rugosus</i>	Regan	1913	26
<i>C. velifer</i>	Meisner	1974	83
<i>C. panticapaei</i>	Shandikov	1995	72
<i>C. aelitae</i>	Shandikov	1995	3
<i>C. bospori</i>	Shandikov	1995	5
<i>C. irinae</i>	Shandikov	1995	23
<i>C. mithridatis</i>	Shandikov	2008	29
<i>C. richardsoni</i>	Shandikov	2011	18

Species considered valid by Nikolaeva (2021) are marked in bold. The last column specifies the minimum number of specimens present in museum collections, based on the GBIF database (<https://www.gbif.org>) and a literature review.

To address a felt demand for a “complete overhaul” (Duhamel, Gasco, & Davaine, 2005; Eastman & Eakin, 2021) of the systematics of the genus *Channichthys*, Nikolaeva and Balushkin began a series of investigations based on comprehensive comparisons of specimens in the collections of the Zoological Institute of the Russian Academy of Sciences in Saint Petersburg, the Ukrainian National Museum of Natural History in Kyiv, and the British Natural History Museum in London. Their analyses indicated that the duplicate gill rakers observed in *C. rhinocerus*, *C. panticapaei*, *C. bospori*, and *C. irinae*, but also in more distantly related icefishes, are a rather labile character (Balushkin & Nikolaeva, 2015), leading them to suggest the synonymization

of the latter three *Channichthys* species (Nikolaeva, 2019). Their work further resulted in redescrptions of *C. velifer* (Nikolaeva & Balushkin, 2019), *C. rhinocerotus* (Nikolaeva, 2020), and *C. rugosus* (Nikolaeva, 2021), as well as the suggested synonymization of *C. aelitae*, *C. mithridatis*, and *C. richardsoni* with *C. rhinocerotus* (Nikolaeva, 2020).

Thus, according to Nikolaeva and Balushkin, the following four species are currently recognized in the genus *Channichthys*: *C. rhinocerotus*, *C. rugosus*, *C. velifer*, and *C. panticapaei*. The redescrbed *C. rugosus* differs from *C. rhinocerotus* in four characters: greater height of the anterior dorsal fin, a fin membrane extending to the apexes of the longest rays, a narrower and concave interorbital space, and a more uniformly reddish body color (Nikolaeva, 2021). *Channichthys rugosus* can be further distinguished from *C. velifer* by numbers of fin rays in the first dorsal and the pectoral fin, bone plaques on the lateral line, and its coloration. Additionally, *C. panticapaei* was said to differ from *C. rugosus* in having a duplicated row of gill rakers and a more brownish-black coloration (Nikolaeva, 2021).

To complement the morphological analyses of *Channichthys* species and further test their validity, genetic data would be essential. Unfortunately, however, molecular information is so far only available for a single species, *C. rhinocerotus*. The genetic data available for this species include a set of ten nuclear markers commonly used in phylogenetic studies, cytochrome c oxidase I (*CO1*) barcodes (Smith et al., 2012), and the recently published complete sequence of a mitochondrial genome with a length of 17,408 bp (Andriyono et al., 2019), as well as restriction-site associated DNA (RAD) markers (Near et al., 2018). These sequences are available from the National Center for Biotechnology Information (NCBI). For the other three potentially valid species of the genus, the unavailability of sequence information is at least in part due to the rarity of suitable tissue samples. To the best of our knowledge no more than 3–72 specimens are present for these species in museum collections (Table 1). Moreover, most specimens of these species were caught decades ago and fixed in formalin, which leads to degradation and chemical modification of DNA, making the recovery of genetic information challenging. To overcome this limitation, protocols for DNA extraction and sequencing library preparation tailored for formalin-fixed specimens have recently become available and proved to be remarkably successful (Gansauge, Aximu-Petri, Nagel, & Meyer, 2020; Gansauge et al., 2017; Gould, Fritts-Penniman, & Gaisner, 2021).

Here, we apply recently developed methods to retrieve DNA sequences from a specimen of *C. rugosus* that was collected and formalin-fixed in 1974, and stored in 70 percent ethanol since. Modifications to a standard DNA extraction protocol from animal tissue maximise the yield of short DNA fragments, while application of a single-stranded DNA library preparation method (Gansauge et al., 2020, 2017) allows to convert even minute amounts of degraded DNA into sequencing libraries. We reconstruct the complete sequence of the specimen's mitochondrial genome based on Illumina read data, and compare this sequence to the mitochondrial genome of *C. rhinocerotus* to assess the genetic divergence

between these two species. We find that the two mitochondrial genomes are nearly identical, with only 27 nucleotide differences between them. Such close similarity lends support to the synonymy of the two species *C. rugosus* and suggests that, like *Pogonophryne*, *Channichthys* comprises fewer differentiated species than previously thought.

## 2 Materials and methods

### 2.1 Sampling

The *C. rugosus* specimen used for sequencing was collected on 28.06.1974 during voyage 7 of the Soviet scientific trawler ‘Skif’ (‘Скиф’). It was obtained by bottom-trawling (trawl 188) on the Kerguelen shelf, at a depth of 115–120 m to the North-East of the Kerguelen Islands (48°34’1 S, 70°37’1 E). The specimen (ZIN 56294) has a standard length of 252 mm and is located in the collection of the Zoological Institute of the Russian Academy of Sciences in Saint Petersburg, Russia. It was formalin-fixed upon arrival in Saint Petersburg and remained in 40% formalin for several years before being transferred to 70% ethanol. The specimen had been identified as *C. rugosus* based on the height of its first dorsal fin, the shape of its interorbital space, its body coloration, numbers of fin rays, and the absence of a second row of gill rakers on the first gill arch (Nikolaeva, 2021).



**Figure 1** *Channichthys rugosus* specimen ZIN 56294. Photograph (a) and x-ray image (b) of the *C. rugosus* specimen used for DNA extraction. The specimen has a standard length of 252 mm.

## 231 **2.2 DNA extraction and sequencing**

232 A small piece of muscle tissue (5.8 mg dry weight) was dried in a vacuum cen-  
233 trifuge and immersed in lysis buffer (260  $\mu$ L ATL buffer (Qiagen) and 40  $\mu$ L  
234 Proteinase K [20 mg/mL]). Two extraction negative control reactions received  
235 the same lysis buffer, but did not contain sample. After 24 h incubation at 56  
236  $^{\circ}$ C, the lysates were centrifuged at 17,000  $\times$  g for 5 minutes and 300  $\mu$ L su-  
237 pernatant mixed with 3000  $\mu$ L Buffer PB (Qiagen). The mixtures were loaded  
238 onto Minelute silica columns (Qiagen) in steps of 600  $\mu$ L, then washed twice  
239 with 600  $\mu$ L Buffer PE (Qiagen). Centrifugation was carried out for 1 minute  
240 each at 8,000  $\times$  g, which is lower than recommended by the manufacturer, in  
241 order to increase the retention of short DNA fragments. The columns were dry  
242 spun 1 minute at 16'000  $\times$  g to remove residual wash buffer. To elute the DNA,  
243 50  $\mu$ L Buffer AE (Qiagen) were placed directly onto the silica membrane, in-  
244 cubated for 10 minutes and centrifuged at 16,000  $\times$  g for 2 minutes. DNA  
245 concentration was determined using 5  $\mu$ L of the extract in a Qubit dsDNA  
246 High Sensitivity assay. The sample yielded 6.6 ng/ $\mu$ L, while the extraction  
247 negatives contained 0.0244 ng/ $\mu$ L or were below the detection threshold of  
248 0.02 ng/ $\mu$ L, respectively. Eight  $\mu$ L of the extract (=52.8 ng DNA) and 30  $\mu$ L  
249 each of the negative controls were then used to build Illumina sequencing li-  
250 braries by single-stranded DNA library preparation as described by [Gansauge](#)  
251 [et al. \(2020, 2017\)](#), using the same reagents as listed in [Gansauge et al. \(2020\)](#).  
252 Briefly, the DNA extract and two extraction negative controls, along with  
253 one library negative control (water) and one library positive control (0.1 pmol  
254 of oligonucleotide CL104) were used for five separate library build reactions.  
255 Furthermore, all reactions received 10 amol CL104 as internal control. Sam-  
256 ples were dephosphorylated and the 3'-adapter (TL181/TL110) attached by  
257 splinted ligation. Adapter molecules were bound to streptavidin-coated mag-  
258 netic beads which were carried through the reactions and washed after each  
259 enzymatic reaction. An adapter-complementary primer (CL128) was used to  
260 prime the fill-in reaction, creating 5'-blunt-ended double stranded molecules.  
261 Another ligation attached the second adapter (CL53/TL178). Libraries were  
262 eluted into 50  $\mu$ L Tween-20 supplemented Tris-EDTA buffer (i.e. TET buffer)  
263 by heat denaturation. 1  $\mu$ L each of a 1:50 dilution of libraries was used in two  
264 qPCR assays to determine control molecule numbers and required PCR-cycle  
265 numbers for amplification. The remaining 49  $\mu$ L of libraries, with the exception  
266 of the positive library control, were then uniquely dual indexed (7 bp index  
267 length) ([Kircher, Sawyer, & Meyer, 2012](#)) and amplified until the end of the  
268 exponential phase, then purified using the Minelute PCR purification kit (Qi-  
269 agen). Libraries were pooled and size-selected to 160–250 bp on a Blue Pippin  
270 instrument using a 3% cassette with internal markers. The selected size frac-  
271 tion was measured with both, the Qubit dsDNA High Sensitivity assay and  
272 the TapeStation HS1000 assay to adjust the input molarity for the sequenc-  
273 ing run. The pool was then sequenced on an Illumina NextSeq500 instrument  
274 using a high-output single-end 75 bp read length kit with custom primers for  
275 read 1 (CL72) and index 2 (Gesaffelstein) ([Paijmans et al., 2017](#)).  
276

Raw read files were demultiplexed using bcl2fastq v.2.19.1 ([https://support.illumina.com/sequencing/sequencing\\_software/bcl2fastq-conversion-software.html](https://support.illumina.com/sequencing/sequencing_software/bcl2fastq-conversion-software.html)), allowing for a maximum combined distance of 1 between barcodes, and saved to fastq format. In the same step, prevalent adapter sequences were trimmed from the ends of reads, and reads under 20 bp of length were omitted.

To ensure the presence of endogenous reads, we matched each read to the NCBI non-redundant (NR) sequence database (downloaded on 12 February 2022) with the BLASTX algorithm as implemented in Diamond v.2.0.4 (Altschul, Gish, Miller, Myers, & Lipman, 1990; Buchfink, Xie, & Huson, 2015). The resulting taxon assignments were plotted with MEGAN v.6.21.4 (Huson et al., 2016).

### 2.3 Reference-based sequence analysis

We mapped reads to the *C. rhinocerotus* mitochondrial genome (Genbank accession number NC.057120) using BWA v.0.7.17 (Li & Durbin, 2010), with its “aln” algorithm and the maximum fraction of missing alignments set to 0.05. The *C. rhinocerotus* mitochondrial genome was obtained from an individual that was collected in 2018 from Antarctic Subarea 58.5.2 (Heard Island and McDonald Island; Sapto Andriyono and Hyun-Woo Kim, priv. comm.). Resulting alignments were filtered to a Phred-scaled mapping quality of 25 or higher with Samtools v.1.9 (Li et al., 2009). Duplicated reads, e.g. from PCR duplicates, were flagged with Picard’s v.2.21.3 (<http://broadinstitute.github.io/picard/>) MarkDuplicate function and filtered with Samtools. Sites with a minimum read depth of 3 were consensus called using ANGSD v.0.933 (Korneliussen, Albrechtsen, & Nielsen, 2014). To recover the terminal positions of the sequence, the first 200 bp of the reference were cut and appended, and the mapping repeated. Regions of low-complexity and larger repeats exceeding the read length were edited manually or replaced with “N” for the length of the reference, as described in the Results section. The degradation state of DNA was assessed by inspection of the distribution of read lengths and analysis of substitution frequencies per base position within reads, using mapDamage v.2.0.8 (Jónsson, Ginolhac, Schubert, Johnson, & Orlando, 2013).

### 2.4 Reference-independent sequence analysis

To exclude potential reference bias, we also performed analyses of the mitochondrial genome of *C. rugosus* based on *de novo* assembly. We performed local assembly of individual mitochondrial markers with aTRAM v.2.0 (Allen, LaFrance, Folk, Johnson, & Guralnick, 2018). As queries, we used nucleotide and protein sequences from all mitochondrial genomes available on NCBI. To identify these notothenioid mitochondrial genomes on NCBI, we used the search string ““Notothenioidi”[Organism] AND (“mitochondrial”[Title] OR “mitochondrion”[Title]) AND “complete genome”[Title]” on 4 December 2021. This set of mitochondrial genomes included the one for *Channichthys*

323 *rhinoceratus* and 40 other unique mitochondrial genomes. From each of these  
324 41 mitochondrial genomes, we extracted each gene (rRNA, tRNA, or protein-  
325 coding) in nucleotide format, and protein-coding features in amino-acid format,  
326 and used all of these in aTRAM analyses. All aTRAM analyses were performed  
327 separately with seven different e-value thresholds (1e-2, 1e-3, 1e-4, 1e-5, 1e-6,  
328 1e-8, 1e-10) for the BLASTN and TBLASTN v.2.10.1 (Altschul et al., 1990)  
329 searches that aTRAM runs internally. As the assembler tool internally em-  
330 ployed by aTRAM, we selected Trinity v.2.10.0 (Grabherr et al., 2011). Each  
331 aTRAM analysis was continued for 20 iterations.

332 All contigs produced by aTRAM were jointly used as input for a sec-  
333 ond assembler tool, MIRA v.4.9.6 (Chevreux, Wetter, & Suhai, 1999). We  
334 set MIRA’s “nasty repeat ratio” to 25 (“-KS:nrr=25”), the “maximum  
335 megahub ratio” to 40 (“-SK:mmhr=40”), specified the lack of quality in-  
336 formation (“-AS:epoq=no”), and turned off the checks for average coverage  
337 (“-NW:cac=no”) and maximum read name length (“-NW:cmrnl=warn”), ac-  
338 cording to the format of the input data. The contigs produced by MIRA (or  
339 their reverse complements) were then individually aligned to the mitochon-  
340 drial genome for *C. rhinoceratus* with MAFFT v.7.470, using a gap opening  
341 penalty of 2, a gap extension penalty of 1, and the program’s “6merpair” and  
342 “addfragments” options.

343

## 344 2.5 Comparative analyses

345

346 The reference-based and reference-independent mitochondrial genome se-  
347 quences for *C. rugosus* were compared visually using AliView v.1.2.6 (Larsson,  
348 2014). Nucleotide sequences of the 13 protein-coding genes were extracted  
349 from the mitochondrial genome of *C. rugosus* and all other notothe-  
350 nioid mitochondrial genomes and aligned per gene with MAFFT. The 13  
351 alignments were concatenated and a distance matrix was calculated from  
352 the concatenated alignment with the Python script “convert.py” (avail-  
353 able from GitHub: [https://github.com/mmatschiner/supergenes/blob/main/gadidae\\_phylogenomics/src/convert.py](https://github.com/mmatschiner/supergenes/blob/main/gadidae_phylogenomics/src/convert.py)), ignoring all sites with missing data.  
354 The concatenated alignment was further used for maximum-likelihood phy-  
355 logenetic inference with IQ-TREE v.2.1.2 (Minh et al., 2020), applying  
356 the program’s automated substitution model selection and 1000 ultrafast  
357 bootstrap (Minh, Nguyen, & von Haeseler, 2013) iterations.

359 To gain a more complete view of sequence variation in *Channichthys*, we  
360 took advantage of the *CO1* barcode sequences available on NCBI (Smith et  
361 al., 2012). We downloaded these sequences and aligned them together with  
362 the homologous sequences extracted from the mitochondrial genomes of *C.*  
363 *rhinoceratus* and *C. rugosus*, using MAFFT. To illustrate the *CO1* sequence  
364 variation in *Channichthys*, we first applied maximum-likelihood phylogenetic  
365 inference with IQ-TREE and then used the estimated phylogeny jointly with  
366 the sequence alignment to draw a haplotype genealogy graph with the program  
367 Fitchi v.1.1.4 (Matschiner, 2016).

368



## 3 Results

### 3.1 Sequencing

For the *C. rugosus* specimen, a total of 63,158,791 reads passed initial trimming and length filtering. For extraction negative controls 1 and 2 (exneg 1, exneg 2), and library negative control (libneg), the number of reads were 22,393,754, 21,343,774 and 3,080,057, respectively. Analysis with Diamond and MEGAN assigned a substantial proportion of the reads to Notothenioidei and confirmed that these were endogenous (Fig. 4).

### 3.2 Reference-based sequence analysis

Mapping to the *C. rhinoceratus* mitochondrial genome generated 48,313 hits, corresponding to 0.0765% of total reads. After filtering duplicates, 18,687 unique reads were used for further analysis. These reads had an average length of 32.98 bp, with only 0.1% of reads being 70 bp or longer. Figure 2 shows the distribution of read lengths of hits. Negative controls produced 5 (exneg 1), 5 (exneg 2), and 1 unique hit (libneg), which weren't analysed further. The resulting coverage had an average depth of 35.4 and extended over 98.1% of the reference. The alignment showed two apparent gaps in the D-loop and spurious alignments directly adjacent to them, therefore positions 15,192–15,294 and 16,856–17,262, respectively, were called as "N" for the length of the reference. A 14-mer C repeat at reference positions 15,986–15,999 was spanned by two reads only, both indicating an indel with one fewer repeat in *C. rugosus*, which was called manually. Mapped reads showed an elevated rate of C to T changes in both their 3'- and 5'-ends, a pattern of cytosine deamination that is typical for degraded DNA (Fig. 3).

### 3.3 Reference-independent sequence analysis

Assembly with MIRA produced 14 contigs with lengths between 317 and 1471 basepairs (bp) (mean length: 677.4 bp). One of these contigs overlapped fully with another one, and two other contigs overlapped by 13 bp. The total length of the mitochondrial genome covered by these contigs was 9,849 bp. No nucleotide differences were observed between overlapping contigs.

### 3.4 Comparative analyses

Comparison of the reference-based and the reference-independent mitochondrial genome sequences showed that these were completely identical across the 9,849 bp covered by both. Compared to the mitochondrial genome of *C. rhinoceratus*, the reference-based sequence differed at 27 sites (Table 2). Seventeen of these nucleotide differences were within regions also covered by the reference-independent sequence for *C. rugosus*, and all of these were confirmed by that sequence. The differences between the *C. rhinoceratus* and *C. rugosus* mitochondrial genomes included five transitions (two A/C, one G/C, one

369  
370  
371  
372  
373  
374  
375  
376  
377  
378  
379  
380  
381  
382  
383  
384  
385  
386  
387  
388  
389  
390  
391  
392  
393  
394  
395  
396  
397  
398  
399  
400  
401  
402  
403  
404  
405  
406  
407  
408  
409  
410  
411  
412  
413  
414

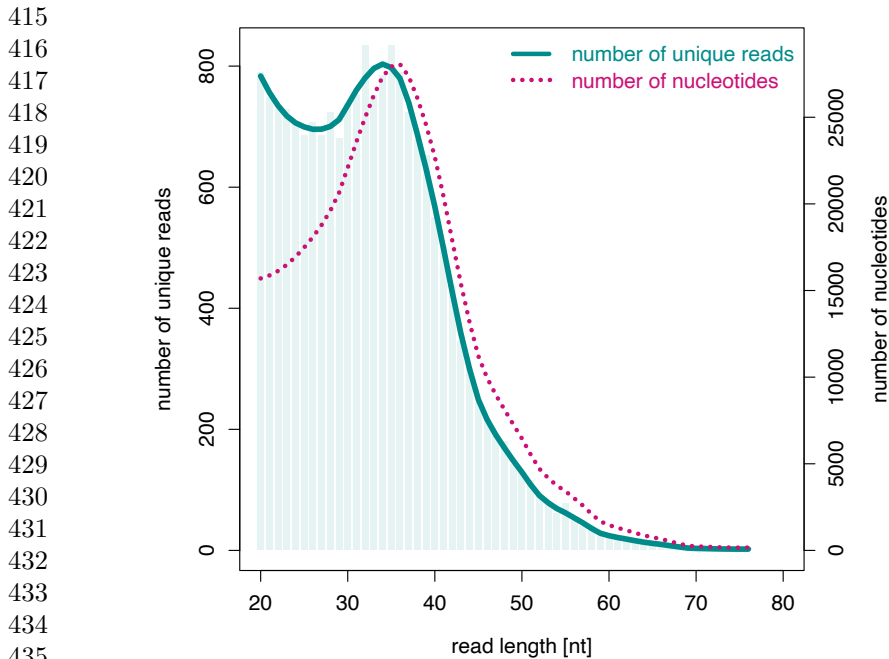


**Figure 2** Distribution of read lengths of hits to the *C. rhinoceratus* mitochondrial genome. The solid line and bars indicate the number of hits for a given read length, the dotted line indicates the amount of data in nucleotides gathered from reads of a given length.

G/T, and one T/G substitution) and 21 transversions (seven A/G, two C/T, six G/A, and six T/C substitutions), as well as one C/- indel. The nucleotide differences were distributed unevenly across the mitochondrial genome and mostly found in the *ND6* gene and the D-loop region (Fig. 5). Compared to the mitochondrial genome-wide background of 0.0011 substitutions per bp, the *ND6*/D-loop region had an elevated divergence of 0.0065 substitutions per bp.

Phylogenetic inference with IQ-TREE based on protein-coding mitochondrial sequences grouped the two *Channichthys* genomes with full bootstrap support. The two taxa were separated only by very short branches that had a combined length of 0.0012 substitutions per bp. The *Channichthys* mitochondrial genomes were most similar to those of *Chionobathyscus dewitti* and *Cryodraco antarcticus*, with which they formed a clade that also received full bootstrap support. This clade appeared as the sister group to a clade formed by the mitochondrial genomes of *Chaenodraco wilsoni* and three members of the genus *Chionodraco*, albeit with low bootstrap support of 70% (Fig. 6).

The haplotype genealogy graph for 14 available *Channichthys CO1* sequences showed that eleven of them shared the same haplotype. Three other haplotypes differed by a single substitution from the majority haplotype and were each represented by a single individual. One of these three private haplotypes was found found in the published mitochondrial genome sequence for

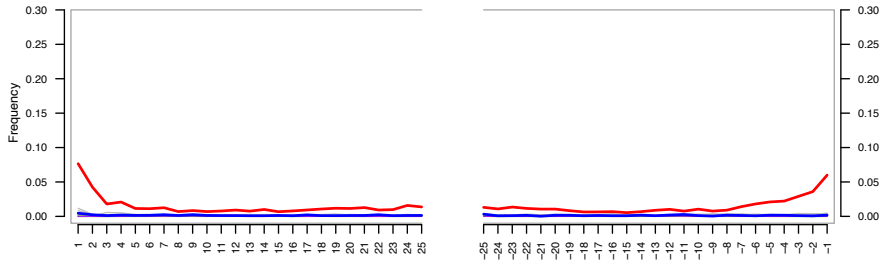


**Figure 3** Frequency of post-mortem C to T changes by nucleotide position within reads. Deaminated cytosines are being read as thymine and are especially prevalent at molecule ends. Red line: relative frequency of T by position in read from 5'-end (left) and 3'-end (right), blue line: relative frequency of A. Here, the deamination signal manifests only as C to T, and not G to A, because single-stranded, rather than double-stranded DNA library preparation was used.

*C. rhinocerotus*, while the *C. rugosus* mitochondrial genome had the majority haplotype (Fig. 7).

## 4 Discussion

Our comparison of the mitochondrial genomes of *C. rhinocerotus* and *C. rugosus* showed that these two mitochondrial genomes are highly similar, with only one indel, 26 nucleotide substitutions and six amino-acid substitutions between them. The sequence divergence is 0.16%, and most of this divergence is concentrated in the *ND6*/D-loop region where the divergence reaches 0.65%. Despite very short read lengths, reconstruction of *C. rugosus*' mitochondrial genome was possible, except for two loci in the *ND6*/D-loop region. Those are most likely repeats that were too large to be spanned by single reads and could not be mapped correctly. While larger rearrangements of nothotenioid mitochondrial genomes have been reported by Papetti et al. (2021), gene order was shown to be identical for eight of the species in figure 6 (all except *Chionobathyscus dewitti*, *Cryodraco antarcticus*, and *Channichthys* sp.). Hence, while possible, the gaps in the alignments are unlikely to be caused by rearrangements or larger indels, and are probably artifacts due to short read length. This highlights a shortcoming of the use of degraded DNA, where read lengths are usually limited by DNA molecule lengths rather than by sequencing technology, making the detection of structural variants challenging.

Analysis of post-mortem damage shows a robust pattern of cytosine deamination in single-stranded overhangs at molecule ends, manifesting as C to T changes in the sequencing data. Given the appreciable depth of coverage, however, we consider it very unlikely that any position was called erroneously due to this damage. Here, only C to T changes are seen as we used single-stranded DNA library preparation. In double-stranded DNA library preparation, deaminated cytosines would also be apparent as G to A changes in the sequencing data. The presence of this deamination signal can be interpreted as evidence for the authenticity of the sequences, as modern contamination would not show

461  
462  
463  
464  
465  
466  
467  
468  
469  
470  
471  
472  
473  
474  
475  
476  
477  
478  
479  
480  
481  
482  
483  
484  
485  
486  
487  
488  
489  
490  
491  
492  
493  
494  
495  
496  
497  
498  
499  
500  
501  
502  
503  
504  
505  
506

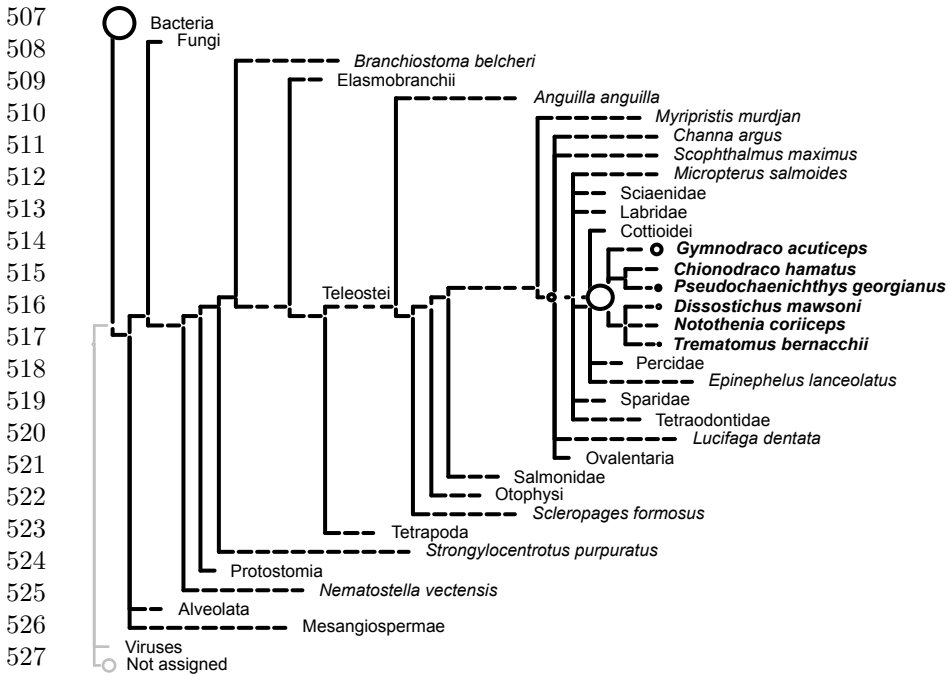


**Figure 4 Taxonomic assignment of individual reads.** Reads were mapped to the NCBI non-redundant (NR) database. The sizes of circles on internal and terminal nodes are proportional to the numbers of reads mapping to the corresponding taxon; a single read mapped to taxa without visible circles.

it. However, this is more relevant for ancient samples, for which the age of endogenous DNA and *ex situ* contamination would be very different, and for cases where contamination is more likely to be confused with endogenous sequences, such as ancient human samples. Here, contamination is unlikely to affect our results, as negative controls didn't produce concerning numbers of reads mapping to the reference, and no other samples or DNA were handled in the laboratory environment which couldn't be readily distinguished from our sample.

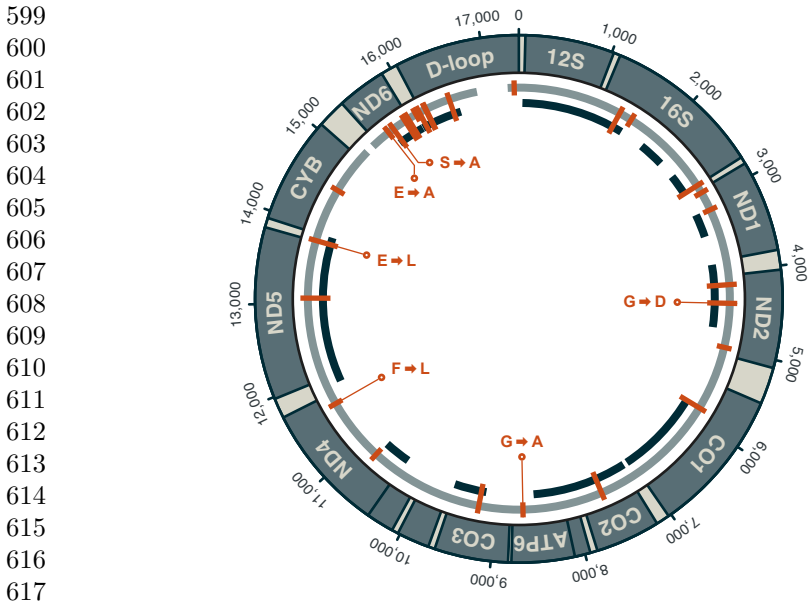
The available molecular data for the genus *Channichthys* does not allow us to perform a formal genetic species delimitation analysis as was recently done for *Pogonophryne* (Parker et al., 2022). Nevertheless, a comparison of the divergence between the two *Channichthys* mitochondrial genomes with the levels of between- and within-species sequence divergence in other notothenioid fishes can inform about the existence of one or several species within the genus. As shown in Fig. 6, the divergence within *Channichthys* is far smaller than that between any other pairs of *Channichthyidae* species. Besides *Channichthys rhinoceratus* and *C. rugosus*, the most closely-related species (judged on the basis of their mitochondrial genomes) appear to be *Chionodraco hamatus* and *Chionodraco rastrispinosus*. However, despite their recent divergence around

**Table 2** Nucleotide substitutions and indel between *Channichthys* mitochondrial genomes

Site	Nucleotide substitution	Codon position	Codon substitution	Amino-acid substitution
1379	a/g			
1552	c/t			
2784	a/g			
2893	a/g	3	cta/ctg	
3145	g/c	3	ctg/ctc	
4165	t/c	3	att/atc	
4410	g/a	2	ggc/gac	G/D
4994	a/g	1	acc/gcc	T/A
5857	g/a	3	tgg/tga	
7586	a/g	3	gaa/gag	
8650	g/a	2	ggc/gac	G/A
9234	t/c	3	ctt/ctc	
10761	g/a	3	acg/aca	
11617	t/c	1	ttt/ctt	F/L
13006	t/c	3	gct/gcc	
13832	g/a	1	gag/aag	E/L
14550	a/c	3	gga/ggc	
15568	t/g	2	gag/gcg	E/A
15647	a/c	1	tca/gca	S/A
15831	a/g	3	gct/gcc	
15882	a/g	3	tgt/tgc	
15999	c/-			
16049	c/t			
16138	g/t			
16147	g/a			
16477	t/c			
17347	t/c			

a million years ago (Colombo, Damerau, Hanel, Salzburger, & Matschiner, 2015), the mitochondrial genomes of these two species are connected by a total branch length of 0.019 substitutions per bp, around 16 times as long as the branches connecting the two *Channichthys* mitochondrial genomes. Of note, the two *Chionodraco* species appear not to be fully separated, given that hybrids and signals of introgression have been observed (Schiaffon et al., 2021).

On the other hand, the divergence between the two *Channichthys* mitochondrial genomes is comparable to the within-species divergence in other notothenioid species. Mitochondrial genomes of two individuals are available for five notothenioid species: *Trematomus borchgrevinkii*, *Notothenia coriiceps*, *Notothenia rossi*, *Chaenodraco wilsoni*, and *Chionodraco hamatus*. These two genomes per species differ by 16–92 substitutions and 3–22 indels across the mitochondrial genome, or by 11–69 substitutions and 2–10 indels when the *ND6* / D-loop region is excluded (Table 3). The divergence of the two *Channichthys* mitochondrial genomes is close to or below the lower ends of these ranges, considering that we found these two genomes to differ in 26 nucleotide substitutions (17 outside the *ND6* / D-loop region) and no indels



618 **Figure 5 Mitochondrial genome of *C. rugosus*.** Coordinates on the outside of the  
619 circle are given in units of basepairs. The gray inner circle indicates the nearly full coverage  
620 achieved in the reference-based analysis. Two gaps with a total length of 510 bp remain  
621 in this sequence between positions 15,192 and 15,294, and between positions 16,856 and  
622 17,262. The black fragments inside the gray circle show the positions of contigs from the  
623 reference-independent approach. Substitutions compared to the mitochondrial genome of  
624 *C. rhinoceratus* (NCBI accession NC\_057120) are marked in orange, and non-synonymous  
625 substitutions are labelled with the resulting amino-acid change.

626 were observed. In contrast, the two most-closely related pairs of sister species  
627 within Channichthyidae (*Chionodraco hamatus*, *Chionodraco rastrospinosus*,  
628 and *Chionobathyscus dewitti*, *Cryodraco antarcticus*; Fig. 2) differ by 421–540  
629 substitutions and 25–34 indels (253–272 substitutions and 6–11 indels when the  
630 *ND6* / D-loop region is excluded; Table 3). Thus, the divergence of the mito-  
631 chondrial genomes of *Channichthys rhinoceratus* and *C. rugosus* is consistent  
632 with the existence of a single species within the genus *Channichthys* (Eastman  
633 & Eakin, 2021). If this result should be confirmed by further molecular data,  
634 *Channichthys rugosus* may need to be synonymized with *C. rhinoceratus*.

635 Low divergence in mitochondrial genome sequence can be indicative of  
636 a close – e.g. intraspecific – phylogenetic relationship, but could also be  
637 due to alternative scenarios. Mitochondrial capture, where one lineage fixes  
638 the mitochondrial genome received from another by introgression, can result  
639 in two valid, reproductively largely isolated species with appreciable  
640 nuclear genome divergence having no or little mitochondrial genome diver-  
641 gence. This phenomenon can also apply to large, rapidly diversifying clades  
642 where many species have arisen from nuclear genomic diversity created through  
643 hybridisation of divergent ancestral lineages, for example in Lake Victoria’s  
644

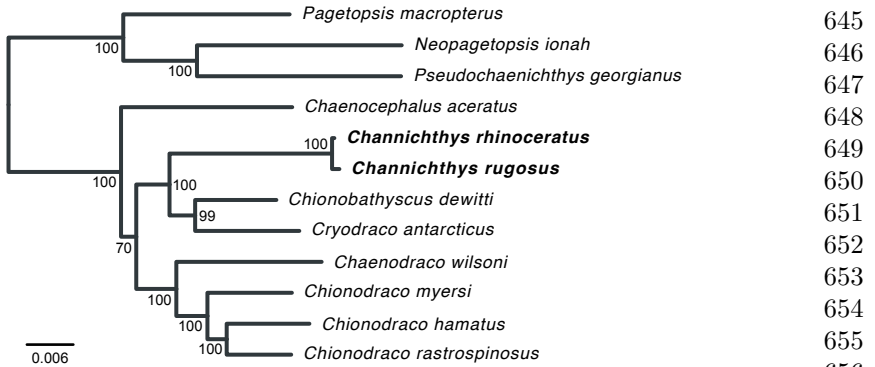


**Figure 6 Mitochondrial phylogeny of Channichthyidae.** Maximum-likelihood phylogeny of all available mitochondrial genomes for Channichthyidae. Short branches connect *Channichthys rhinoceras* and *C. rugosus*.

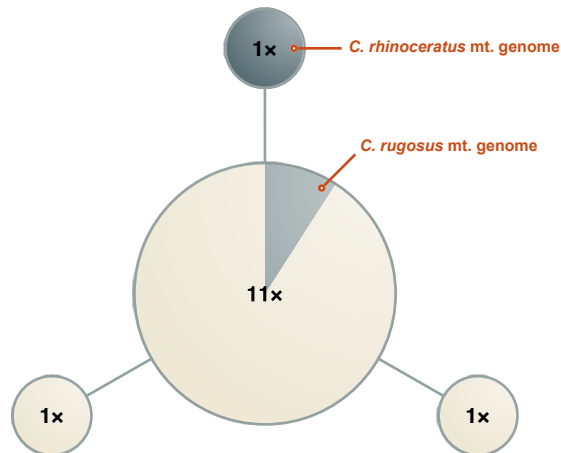


**Figure 7 Haplotype genealogy graph for CO1.** Circles represent four distinct *Channichthys* CO1 haplotypes, found in 13 *C. rhinoceras* and one *C. rugosus* individuals. Radii are drawn according to the number of individuals with that haplotype (indicated with labels on circles). Edges represent substitutions. Each of the three edges has a length of one substitution. mt., mitochondrial.

haplochromine cichlids (Meier et al., 2017). In that case low mitochondrial diversity and rampant haplotype sharing would conceal a large species diversity. It would need to be tested using genome-wide nuclear data if such a scenario applies to *Channichthys*, rather than a previous overestimation of species diversity in the genus.

Genetic data can be vital to corroborate or reject taxonomic assessments based on morphology and to more accurately estimate organismal diversity. The fixation of specimens with formalin, which severely hampers genetic analyses, has long been recognized, and indeed lamented, as a major obstacle for tapping the theoretically vast potential of museum collections for addressing

**Table 3** Within-species mitochondrial sequence divergence in Notothenioidei and between-species divergence for closely-related Channichthyidae

Species	Accessions	# s.	# i.	# s. <sup>1</sup>	# i. <sup>1</sup>
<i>Trematomus borchgrevinki</i>	NC_030320, KX025131	92	22	69	8
<i>Notothenia coriiceps</i>	NC_015653, AP006021	16	3	12	2
<i>Notothenia rossii</i>	NC_050685, MT192936	22	15	11	4
<i>Chaenodraco wilsoni</i>	NC_039158, MT559885	48	11	33	10
<i>Chionodraco hamatus</i>	NC_029737, KU341409	55	13	42	5
<i>Chionodraco hamatus</i> , <i>Chionodraco rastrorpinosus</i>	NC_029737, NC_039543	421	25	253	6
<i>Chionobathyscus dewitti</i> , <i>Cryodraco antarcticus</i>	NC_046762, NC_045285	540	34	272	11
<i>Channichthys rhinoceratus</i> , <i>Channichthys rugosus</i>	NC_057120, new	26 <sup>2</sup>	0 <sup>2</sup>	17	0

s., substitutions; i., indels.

<sup>1</sup>Excluding the *ND6* / D-loop region.

<sup>2</sup>Potentially incomplete due to two gaps in the *C. rugosus* sequence within the *ND6* / D-loop region.

long standing questions in systematics, taxonomy, evolutionary and conservation biology (Card, Shapiro, Giribet, Moritz, & Edwards, 2021; Raxworthy & Smith, 2021). Time-structured samples, including extinct species, can reveal details about the recent decline of biodiversity. Specimens from places that are difficult to access could fill gaps in studies otherwise relying on a smaller geographic sampling. Given this potential it is unsurprising that the research community continues to undertake great efforts in refining methodology to maximise the data yield from wet-collection specimens (Campos & Gilbert, 2012; Hahn et al., 2021; Hykin, Bi, & Mcguire, 2015; Schander & Kenneth, 2003; Straube et al., 2021). Here, we demonstrated that recently proposed methods that build on advances in the study of ancient DNA and high-throughput shotgun sequencing can recover usable genetic data from a formalin-fixed fish specimen. The short molecule lengths and very low DNA amounts recovered from such samples mandate the use of specialised, sensitive methods, such as lower centrifugation speeds and greater excess of binding buffer in DNA extraction (Dabney et al., 2013). The chemical cross-linking of DNA with DNA and proteins requires a harsher treatment of the tissue sample during lysis, for example by using high amounts of proteinase, as done here. Subsequently, the use of very efficient single-stranded DNA library preparation can convert appreciable numbers of molecules even if chemical damage and cross-linking are prevalent. Caution should be taken when analysing such low-yield samples, as levels of contamination regarded minor in other circumstances can obscure signal from the target or lead to incorrect interpretations. Working in a clean laboratory that is dedicated to the analysis of low-biomass,



degraded samples is therefore recommended, as well as including appropriate negative controls to monitor contamination. This extra effort, however, is greatly rewarded when open questions can be addressed with otherwise unobtainable data.

**Code Availability.** Analysis code is available from GitHub (<https://github.com/mmatschiner/unsequenced>).

**Acknowledgments.** We thank Arcady V. Balushkin for providing the *C. rugosus* specimen and Marcelo Sánchez-Villagra for financially supporting the sequencing of its mitochondrial genome. Supto Andriyono and Hyun-Woo Kim provided helpful information about the *C. rhinoceratus* mitochondrial genome. Mark Lever (ETH Zurich) kindly provided lab space. The Genetic Diversity Centre (ETH Zurich) provided access to laboratory and HPC facilities. The Functional Genomics Centre Zürich (ETH and University of Zurich) provided assistance with sequencing.

**Author Contributions.** M.Mu. performed molecular lab work, bioinformatic analyses, and contributed to the manuscript. E.N. initiated the study and contributed the tissue sample of *C. rugosus*. L.R. established the collaboration. M.Ma. performed bioinformatic analyses and wrote most of the manuscript. All authors read and approved the final version of the manuscript.

**Funding.** M. Muschick was supported by the SNSF Sinergia grant CR-SII5\_183566. M. Matschiner was supported by the Norwegian Research Council with FRIPRO grant 275869. E. Nikolaeva was supported by a research programme of the Zoological Institute of the Russian Academy of Sciences (project number 122031100285-3).

## Declarations

**Conflict of interest.** The authors declare that no competing interest exists, as well as that there is no financial support or relationships that may pose any kind of conflict. Likewise, the authors declare that contributed to the text, agreed with its content and approved it for submission.

## References

- Allen, J.M., LaFrance, R., Folk, R.A., Johnson, K.P., Guralnick, R.P. (2018). aTRAM 2.0: An improved, flexible locus assembler for NGS data. *Evolutionary Bioinformatics*, 14, 1176934318774546.  
10.1177/1176934318774546
- Altschul, S.F., Gish, W., Miller, W., Myers, E.W., Lipman, D.J. (1990). Basic local alignment search tool. *Journal of Molecular Biology*, 215(3), 403–410.

- 783  
784 10.1016/s0022-2836(05)80360-2  
785
- 786 Andriyono, S., Alam, M.J., Lee, S.R., Choi, S.-G., Chung, S., Kim, H.-W.  
787 (2019, July). Characterization of the complete mitochondrial genome of  
788 *Chionobathyscus dewitti* (Perciformes, Channichthyidae). *Mitochondrial*  
789 *DNA Part B*, 4(2), 3914–3915.
- 790  
791 10.1080/23802359.2019.1688112
- 792  
793 Balushkin, A.V., & Nikolaeva, E.A. (2015). “Dolichobranchiata” muta-  
794 tion in the Antarctic representatives from the families of plunderfishes  
795 (Artedidraconidae) and white-blooded (Channichthyidae) fish (Notothe-  
796 nioidei). *Journal of Ichthyology*, 55(1), 9–15.
- 797  
798 10.1134/S0032945215010014
- 799  
800 Buchfink, B., Xie, C., Huson, D.H. (2015). Fast and sensitive protein alignment  
801 using DIAMOND. *Nature Methods*, 12(1), 59–60.
- 802  
803 10.1038/nmeth.3176
- 804  
805 Campos, P.F., & Gilbert, T.M.P. (2012). DNA extraction from formalin-fixed  
806 material. *Methods in molecular biology (Clifton, N.J.)*, 840, 81–5.
- 807  
808 10.1007/978-1-61779-516-9\11
- 809  
810 Card, D.C., Shapiro, B., Giribet, G., Moritz, C., Edwards, S.V. (2021).  
811 Museum Genomics. *Annual Review of Genetics*, 55(1), 1–27.
- 812  
813 10.1146/annurev-genet-071719-020506
- 814  
815 Chevreux, B., Wetter, T., Suhai, S. (1999). Genome sequence assembly using  
816 trace signals and additional sequence information. *Computer Science*  
817 *and Biology: Proceedings of the German Conference on Bioinformatics*  
818 *(GCB)*, 1–12.
- 819  
820 Clarke, A., & Johnston, I.A. (1996). Evolution and adaptive radiation of  
821 antarctic fishes. *Trends in Ecology and Evolution*, 11(5), 212–218.
- 822  
823 10.1016/0169-5347(96)10029-X
- 824  
825 Colombo, M., Damerou, M., Hanel, R., Salzburger, W., Matschiner, M.  
826 (2015). Diversity and disparity through time in the adaptive radiation  
827 of Antarctic notothenioid fishes. *Journal of Evolutionary Biology*, 28(2),  
828 376–394.

	829
10.1111/jeb.12570	830
	831
Dabney, J., Knapp, M., Glocke, I., Gansauge, M.-T., Weihmann, A., Nickel, B., ... Meyer, M. (2013, 09). Complete mitochondrial genome sequence of a Middle Pleistocene cave bear reconstructed from ultrashort DNA fragments. <i>Proceedings Of The National Academy Of Sciences Of The United States Of America</i> , 110(39), 15758 – 15763.	832
	833
	834
	835
	836
	837
10.1073/pnas.1314445110	838
	839
Duhamel, G., Gasco, N., & Davaine, P. (Eds.). (2005). <i>Poissons des Îles Kerguelen et Crozet. Guide Régional de l’Océan Austral. Patrimoines Naturels</i> (Vol. 63). Paris: Muséum National d’Histoire Naturelle.	840
	841
	842
Eastman, J.T. (2005). The nature of the diversity of Antarctic fishes. <i>Polar Biology</i> , 28(2), 93–107.	843
	844
	845
	846
10.1007/s00300-004-0667-4	847
	848
Eastman, J.T., & Eakin, R.R. (2021). Checklist of the species of notothenioid fishes. <i>Antarctic Science</i> , 33(3), 273–280.	849
	850
	851
10.1017/S0954102020000632	852
	853
Gansauge, M.-T., Aximu-Petri, A., Nagel, S., Meyer, M. (2020). Manual and automated preparation of single-stranded DNA libraries for the sequencing of DNA from ancient biological remains and other sources of highly degraded DNA. <i>Nature Protocols</i> , 15(8), 2279–2300.	854
	855
	856
	857
	858
10.1038/s41596-020-0338-0	859
	860
Gansauge, M.-T., Gerber, T., Glocke, I., Korlević, P., Lippik, L., Nagel, S., ... Meyer, M. (2017). Single-stranded DNA library preparation from highly degraded DNA using T4 DNA ligase. <i>Nucleic Acids Research</i> , gkx033.	861
	862
	863
	864
10.1093/nar/gkx033	865
	866
Gon, O., & Heemstra, P.C. (1990). <i>Fishes of the Southern Ocean</i> . Grahamstown, South Africa: J.L.B. Smith Institute of Ichthyology. (Pages: 196)	867
	868
	869
Gould, A.L., Fritts-Penniman, A., Gaisner, A. (2021). Museum genomics illuminate the high specificity of a bioluminescent symbiosis for a genus of reef fish. <i>Frontiers in Ecology and Evolution</i> , 9, 630207.	870
	871
	872
	873
10.3389/fevo.2021.630207	874

- 875 Grabherr, M.G., Haas, B.J., Yassour, M., Levin, J.Z., Thompson, D.A., Amit,  
876 I., . . . Regev, A. (2011). Full-length transcriptome assembly from RNA-  
877 Seq data without a reference genome. *Nature Biotechnology*, *29*(7), 644–  
878 652.  
879  
880 10.1101/gr.229202
- 881  
882 Hahn, E.E., Alexander, M.R., Greal, A., Stiller, J., Gardiner, D.M., Holleley,  
883 C.E. (2021). Unlocking inaccessible historical genomes preserved in  
884 formalin. *Molecular Ecology Resources*.  
885  
886 10.1111/1755-0998.13505
- 887  
888 Hureau, J.-C. (1964). Sur la probable identité des deux espèces du genre  
889 *Chaenichthys*, de la famille des Channichthyidae (poissons à "sang  
890 blanc"). *Bulletin du Muséum National d'Histoire Naturelle*, *36*(4),  
891 450–456.  
892
- 893  
894 Huson, D.H., Beier, S., Flade, I., Górska, A., El-Hadidi, M., Mitra, S., . . .  
895 Tappu, R. (2016). MEGAN Community Edition - interactive explo-  
896 ration and analysis of large-scale microbiome sequencing data. *PLOS*  
897 *Computational Biology*, *12*(6), e1004957.  
898  
899 10.1371/journal.pcbi.1004957
- 900  
901 Hykin, S.M., Bi, K., Mcguire, J.A. (2015). Fixing Formalin:  
902 A Method to Recover Genomic-Scale DNA Sequence Data from  
903 Formalin-Fixed Museum Specimens Using High-Throughput Sequenc-  
904 ing. *PLoS ONE*, *10*(10), e0141579 – 16. Retrieved from  
905 <https://dx.plos.org/10.1371/journal.pone.0141579>  
906  
907 10.1371/journal.pone.0141579
- 908  
909 Jónsson, H., Ginolhac, A., Schubert, M., Johnson, P.L.F., Orlando, L. (2013).  
910 mapDamage2.0: fast approximate Bayesian estimates of ancient DNA  
911 damage parameters. *Bioinformatics*, *29*(13), 1682 – 1684.  
912  
913 10.1093/bioinformatics/btt193
- 914  
915 Kircher, M., Sawyer, S., Meyer, M. (2012). Double indexing overcomes inac-  
916 curacies in multiplex sequencing on the Illumina platform. *Nucleic Acids*  
917 *Research*, *40*(1), e3–e3.  
918  
919 10.1093/nar/gkr771  
920

- Korneliussen, T.S., Albrechtsen, A., Nielsen, R. (2014). ANGSD: Analysis of next generation sequencing data. *BMC Bioinformatics*, 15(1), 356. 921  
922  
923  
10.1186/s12859-014-0356-4 924  
925
- Larsson, A. (2014). AliView: a fast and lightweight alignment viewer and editor for large datasets. *Bioinformatics*, 30(22), 3276–3278. (Publisher: Oxford University Press) 926  
927  
928  
10.1093/bioinformatics/btu531 929  
930  
931
- Li, H., & Durbin, R. (2010). Fast and accurate long-read alignment with Burrows-Wheeler transform. *Bioinformatics*, 26(5), 589 – 595. 932  
933  
934  
10.1093/bioinformatics/btp698 935  
936
- Li, H., Handsaker, B., Wysoker, A., Fennell, T., Ruan, J., Homer, N., ... Subgroup, .G.P.D.P. (2009). The Sequence Alignment/Map format and SAMtools. *Bioinformatics*, 25(16), 2078–2079. 937  
938  
939  
10.1093/bioinformatics/btp352 940  
941  
942
- Matschiner, M. (2016). Fitchi: haplotype genealogy graphs based on the Fitch algorithm. *Bioinformatics*, 32(8), 1250–1252. 943  
944  
945  
10.1093/bioinformatics/btv717 946  
947
- Matschiner, M., Colombo, M., Damerau, M., Ceballos, S., Hanel, R., Salzburger, W. (2015). The adaptive radiation of notothenioid fishes in the waters of Antarctica. *Extremophile Fishes: Ecology, Evolution, and Physiology of Teleosts in Extreme Environments* (Vol. 36). Cham: Springer International Publishing. 10.1111/j.1365-294X.2006.03105.x 948  
949  
950  
951  
952
- Meier, J.I., Marques, D.A., Mwaiko, S., Wagner, C.E., Excoffier, L., Seehausen, O. (2017). Ancient hybridization fuels rapid cichlid fish adaptive radiations. *Nature Communications*, 8, 14363. 953  
954  
955  
10.1038/ncomms14363 956  
957  
958
- Meisner, E.E. (1974). New species of the icefishes from the Southern Ocean. *Vestnik Zoologii*, 6, 50–55. 959  
960  
961  
962
- Minh, B.Q., Nguyen, M.A.T., von Haeseler, A. (2013). Ultrafast approximation for phylogenetic bootstrap. *Molecular Biology and Evolution*, 30(5), 1188–1195. 963  
964  
965  
966

- 967 10.1093/oxfordjournals.molbev.a025811  
 968  
 969 Minh, B.Q., Schmidt, H.A., Chernomor, O., Schrempf, D., Woodhams, M.D.,  
 970 Von Haeseler, A., Lanfear, R. (2020). IQ-TREE 2: New models and  
 971 efficient methods for phylogenetic inference in the genomic era. *Molecular*  
 972 *Biology and Evolution*, 37(5), 1530–1534.  
 973  
 974 10.1093/molbev/msaa015  
 975  
 976 Near, T.J., Dornburg, A., Harrington, R.C., Oliveira, C., Pietsch, T.W.,  
 977 Thacker, C.E., ... Beaulieu, J.M. (2015). Identification of the notothe-  
 978 nioid sister lineage illuminates the biogeographic history of an Antarctic  
 979 adaptive radiation. *BMC Evolutionary Biology*, 15, 109.  
 980  
 981 10.1186/s12862-015-0362-9  
 982  
 983 Near, T.J., Dornburg, A., Kuhn, K.L., Eastman, J.T., Pennington, J.N., Patar-  
 984 nello, T., ... Jones, C.D. (2012). Ancient climate change, antifreeze,  
 985 and the evolutionary diversification of Antarctic fishes. *Proceedings of*  
 986 *the National Academy of Sciences USA*, 109(9), 3434–3439.  
 987  
 988 10.1073/pnas.1115169109  
 989  
 990 Near, T.J., MacGuigan, D.J., Parker, E., Struthers, C.D., Jones, C.D.,  
 991 Dornburg, A. (2018). Phylogenetic analysis of Antarctic notothe-  
 992 nioids illuminates the utility of RADseq for resolving Cenozoic adaptive  
 993 radiations. *Molecular Phylogenetics and Evolution*, 129, 268–279.  
 994  
 995 10.1016/j.ympev.2018.09.001  
 996  
 997 Nikolaeva, E.A. (2019). A review of the icefish species from the genus  
 998 *Channichthys* Richardson, 1844 (Channichthyidae) with double-rowed  
 999 gill rakers. *Proceedings of the Zoological Institute RAS*, 323(4), 558–567.  
 1000  
 1001 10.31610/trudyzin/2019.323.4.558  
 1002  
 1003 Nikolaeva, E.A. (2020). Redescription of the unicorn icefish *Channichthys*  
 1004 *rhinocerotus* Richardson (Notothenioidei: Channichthyidae) with syn-  
 1005 onymization of three similar species. *Proceedings of the Zoological*  
 1006 *Institute RAS*, 324(4), 485–496.  
 1007  
 1008 10.31610/trudyzin/2020.324.4.485  
 1009  
 1010 Nikolaeva, E.A. (2021). On the taxonomic status of the red icefish *Chan-*  
 1011 *nichthys rugosus* (Notothenioidei: Channichthyidae) from the Kerguelen  
 1012 Islands (South Ocean). *Proceedings of the Zoological Institute RAS*, 325,  
 485–494.

	1013
10.31610/trudyzin/2021.325.4.485	1014
	1015
Nikolaeva, E.A., & Balushkin, A.V. (2019). Morphological characteristics of sailfish pike <i>Channichthys velifer</i> (Channichthyidae) from the Kerguelen Islands (Southern Ocean). <i>Journal of Ichthyology</i> , 59(6), 834–842.	1016
	1017
	1018
	1019
10.1134/S0032945219060079	1020
	1021
Norman, J.R. (1937). Fishes. B.A.N.Z. Antarctic Research Expedition 1929–31. <i>Repts Ser B Zool Bot</i> , 1(2), 50–88.	1022
	1023
	1024
	1025
Paijmans, J.L.A., Baleka, S., Henneberger, K., Taron, U.H., Trinks, A., Westbury, M.V., Barlow, A. (2017). Sequencing single-stranded libraries on the Illumina NextSeq 500 platform. <i>arXiv:1711.11004 [q-bio]</i> . Retrieved from <a href="http://arxiv.org/abs/1711.11004">http://arxiv.org/abs/1711.11004</a> (arXiv: 1711.11004)	1026
	1027
	1028
	1029
	1030
Papetti, C., Babbucci, M., Dettai, A., Basso, A., Lucassen, M., Harms, L., ... Negrisolo, E. (2021). Not Frozen in the Ice: Large and Dynamic Rearrangements in the Mitochondrial Genomes of the Antarctic Fish. <i>Genome Biology and Evolution</i> , 13(3), evab017.	1031
	1032
	1033
	1034
	1035
10.1093/gbe/evab017	1036
	1037
Parker, E., Dornburg, A., Struthers, C.D., Jones, C.D., Near, T.J. (2022). Phylogenomic species delimitation dramatically reduces species diversity in an Antarctic adaptive radiation. <i>Systematic Biology</i> , 71(1), 58–77.	1038
	1039
	1040
	1041
10.1093/sysbio/syab057	1042
	1043
Raxworthy, C.J., & Smith, B.T. (2021). Mining museums for historical DNA: advances and challenges in museomics. <i>Trends in Ecology &amp; Evolution</i> , 36(11), 1049–1060.	1044
	1045
	1046
	1047
10.1016/j.tree.2021.07.009	1048
	1049
Regan, C.T. (1913). II. – The Antarctic fishes of the Scottish National Antarctic expedition. <i>Transactions of the Royal Society of Edinburgh: Earth Sciences</i> , 49(2), 229–292.	1050
	1051
	1052
	1053
	1054
Richardson, J. (1844, June). LII.— <i>Descriptions of a new Genus of Gobioid Fish</i> . <i>Annals and Magazine of Natural History</i> , 13(86), 461–462.	1055
	1056
	1057
10.1080/03745484409442631	1058

- 1059 Rüber, L., & Zardoya, R. (2005). Rapid cladogenesis in marine fishes revisited.  
1060 *Evolution*, 59(5), 1119–1127.  
1061  
1062 10.1111/j.0014-3820.2005.tb01048.x  
1063
- 1064 Schander, C., & Kennen, H.M. (2003, 01). DNA, PCR and formalized  
1065 animal tissue – a short review and protocols. *Organisms Diversity &*  
1066 *Evolution*, 3(3), 195–205.  
1067  
1068 10.1078/1439-6092-00071  
1069
- 1070 Schiavon, L., Dulière, V., La Mesa, M., Marino, I.A.M., Codogno, G., Boscari,  
1071 E., ... Papetti, C. (2021). Species distribution, hybridization and con-  
1072 nectivity in the genus *Chionodraco* : Unveiling unknown icefish diversity  
1073 in antarctica. *Diversity and Distributions*, 27(5), 766–783.  
1074  
1075 10.1111/ddi.13249  
1076
- 1077 Shandikov, G.A. (1995a). A new species of icefish, *Channichthys panti-*  
1078 *capei* sp. n. (Channichthyidae, Notothenioidei) from the Kerguelen Island  
1079 (Antarctica). *Proceedings of South Research Institute of Marine Fishery*  
1080 *and Oceanography (YugNIRO), Special Issue, 1*, 1–10.  
1081
- 1082 Shandikov, G.A. (1995b). To the question about the composition of icefish  
1083 species of the genus *Channichthys* in the Kerguelen Islands area with  
1084 description of three new species. *Proceedings of South Research Institute*  
1085 *of Marine Fishery and Oceanography (YugNIRO), Special Issue, 2*, 1–18.  
1086  
1087
- 1088 Shandikov, G.A. (2008). *Channichthys mithridatis*, a new species of icefishes  
1089 (Perciformes: Notothenioidei: Channichthyidae) from the Kerguelen Is-  
1090 lands (East Antarctica), with comments on the taxonomic status of  
1091 *Channichthys normani*. *Visnyk Charkivs'koho Universytetu Imeni V. N.*  
1092 *Karazina, Ser. Biologija, Charkiv*, 14(917), 123–131.  
1093  
1094
- 1095 Shandikov, G.A. (2011). *Channichthys richardsoni* sp. n., a new Antarctic  
1096 icefish (Perciformes: Notothenioidei: Channichthyidae) from the Kergue-  
1097 len Islands area, Indian sector of the Southern Ocean. *Journal of V. N.*  
1098 *Karazin Kharkiv National University, Series: Biology*(14), 125–134.  
1099  
1100
- 1101 Smith, P.J., Steinke, D., Dettai, A., McMillan, P., Welsford, D., Stewart, A.,  
1102 Ward, R.D. (2012, September). DNA barcodes and species identifications  
1103 in Ross Sea and Southern Ocean fishes. *Polar Biology*, 35(9), 1297–1310.  
1104



10.1007/s00300-012-1173-8	1105
	1106
Spodareva, V.V., & Balushkin, A.V. (2014, January). Description of a new species of plunderfish of genus <i>Pogonophryne</i> (Perciformes: Arctidraconidae) from the Bransfield Strait (Antarctica) with a key for the identification of species of the group “marmorata”. <i>Journal of Ichthyology</i> , 54(1), 1–6.	1107
	1108
	1109
	1110
	1111
	1112
10.1134/S0032945214010135	1113
	1114
Straube, N., Lyra, M.L., Paijmans, J.L.A., Preick, M., Basler, N., Penner, J., ... Hofreiter, M. (2021). Successful application of ancient DNA extraction and library construction protocols to museum wet collection specimens. <i>Molecular Ecology Resources</i> , 21(7), 2299–2315.	1115
	1116
	1117
	1118
	1119
10.1111/1755-0998.13433	1120
	1121
	1122
	1123
	1124
	1125
	1126
	1127
	1128
	1129
	1130
	1131
	1132
	1133
	1134
	1135
	1136
	1137
	1138
	1139
	1140
	1141
	1142
	1143
	1144
	1145
	1146
	1147
	1148
	1149
	1150